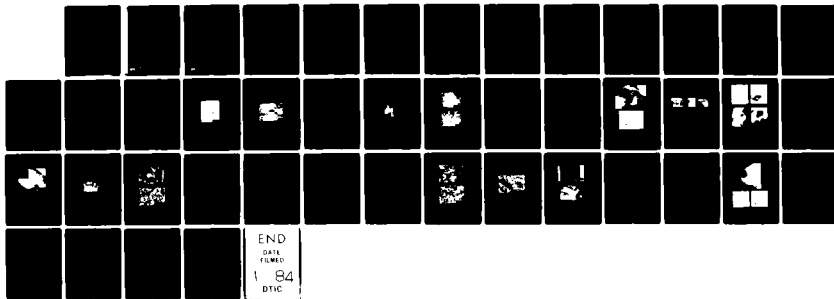


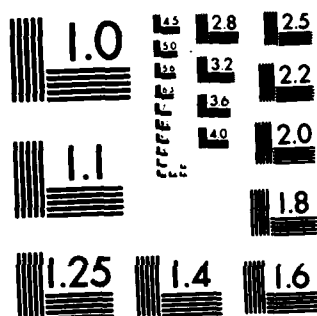
AD-A136 547

SILICON NITRIDE JOINING(U) SRI INTERNATIONAL MENLO PARK 1/1
CA S M JOHNSON ET AL. 31 MAR 83 AFOSR-TR-83-1145
F49620-81-K-0001

UNCLASSIFIED

F/G 11/2 NL





MICROCOPY RESOLUTION TEST CHART
NATIONAL BUREAU OF STANDARDS-1963-A

AFOSR-TR- 32 - 1145

SILICON NITRIDE JOINING

Annual Report

March 1983

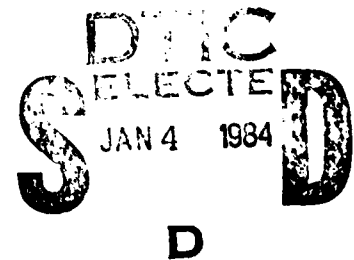
By: S. M. Johnson and D. J. Rowcliffe

Prepared for:

DEPARTMENT OF THE AIR FORCE
Air Force Office of Scientific Research (AFSC)
Bolling Air Force Base, DC 20332
Attention: Dr. A. H. Rosenstein

Contract F49620-81-K-0001

SRI Project PYU 2527



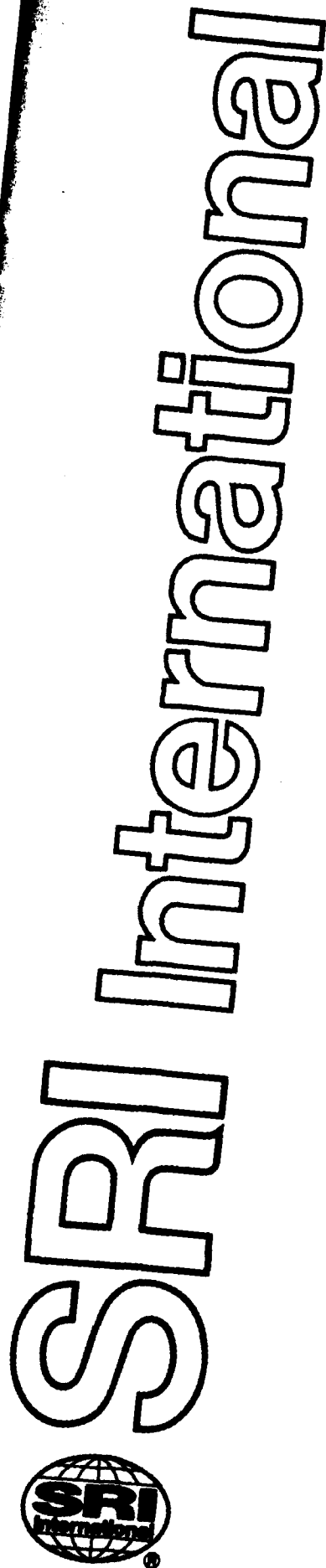
Approved for public release;
distribution unlimited.

SRI International
333 Ravenswood Avenue
Menlo Park, California 94025
(415) 326-6200
TWX: 910-373-2046
Telex: 334 486

DTIC FILE COPY



84 373 2046



SILICON NITRIDE JOINING

Annual Report

March 1983

By: S. M. Johnson and D. J. Rowcliffe

Prepared for:

DEPARTMENT OF THE AIR FORCE
Air Force Office of Scientific Research (AFSC)
Bolling Air Force Base, DC 20332
Attention: Dr. A. H. Rosenstein

Contract F49620-81-K-0001

SRI Project PYU 2527

AIR FORCE OFFICE OF SCIENTIFIC RESEARCH (AFSC)

NOTICE OF TRANSMITTAL TO DTIC

This technical report has been reviewed and is approved for release to the public under the provisions of the DTIC system.

Distribution is unlimited.

MATTHEW J. KLEINER

Chief, Technical Information Division

Approved by:

D. L. Hildenbrand, Director
Materials Research Laboratory

G. R. Abrahamson
Vice President
Physical Sciences Division



Accession For	
NTIS GRA&I	<input checked="" type="checkbox"/>
DTIC TAB	<input type="checkbox"/>
Unannounced	<input type="checkbox"/>
Justification	
By	
Distribution/	
Availability Codes	
Dist	Avail and/or Special
A/1	

UNCLASSIFIED

SECURITY CLASSIFICATION OF THIS PAGE (When Data Entered)

REPORT DOCUMENTATION PAGE		READ INSTRUCTIONS BEFORE COMPLETING FORM	
1. REPORT NUMBER AFOSR-TR-83-1145	2. GOVT ACCESSION NO. A136347	3. RECIPIENT'S CATALOG NUMBER	
4. TITLE (and Subtitle) SILICON NITRIDE JOINING		5. TYPE OF REPORT & PERIOD COVERED ANNUAL REPORT 1-31-82 to 1-31-83	
		6. PERFORMING ORG. REPORT NUMBER PYU 2527	
7. AUTHOR(s) SYLVIA M. JOHNSON DAVID J. ROWCLIFFE		8. CONTRACT OR GRANT NUMBER(s) F49620-81-K-0001	
9. AUTHORING ORGANIZATION NAME(S) AND ADDRESS(ES) SRI International 333 Ravenswood Ave. Menlo Park, CA 94025		10. PROGRAM ELEMENT, PROJECT, TASK AREA & WORK UNIT NUMBERS 61102F 2306/A2	
11. CONTROLLING OFFICE NAME AND ADDRESS AFOSR/NE Dolling HFB, DC-20332		12. REPORT DATE 3-31-83	
14. MONITORING AGENCY NAME & ADDRESS (if different from Controlling Office)		13. NUMBER OF PAGES 36	
		15. SECURITY CLASS (of this report) UNCLASSIFIED	
16. DISTRIBUTION STATEMENT (of this Report) Approved for public release; distribution unlimited.		15a. DECLASSIFICATION/DOWNGRADING SCHEDULE	
17. DISTRIBUTION STATEMENT (of the abstract entered in Block 20, if different from Report)			
18. SUPPLEMENTARY NOTES			
19. KEY WORDS (Continue on reverse side if necessary and identify by block number) SILICON NITRIDE, JOINING STRENGTH, SILICON OXYNITRIDE, TRANSMISSION ELECTRON MICROSCOPY			
20. ABSTRACT (Continue on reverse side if necessary and identify by block number) → Silicon nitride can be joined using an oxide glass which reacts to form a phase similar to the grain boundary phase found in hot pressed Si₃N₄. The microstructure and interfacial reactions were studied by scanning transmission electron microscopy and X-ray diffraction. Silicon nitride dissolves in the glass and silicon oxynitride crystals precipitate. The glass also penetrates the Si₃N₄ and is present as enlarged glass pockets in the bulk ceramic away from the joint. The optimal joining conditions were determined to be 1575-			

DD FORM 1 JAN 73 1473

EDITION OF 1 NOV 65 IS OBSOLETE

UNCLASSIFIED

SECURITY CLASSIFICATION OF THIS PAGE (When Data Entered)

UNCLASSIFIED

SECURITY CLASSIFICATION OF THIS PAGE(When Data Entered)

1650°C and 30 to 60 minutes. The maximum strengths at room temperature determined by 4 point bend tests of bars joined under these conditions were ~ 460 MPa, regardless of the specific conditions. The strength is related to the joint thickness, reaching a maximum for joint thicknesses of ~ 25 to 35 μ m. Two fracture mechanisms were identified by SEM. Silicon oxynitride crystals grow across thin joints and the resulting microstructure is strong if few pores are present. Thermal expansion mismatch cracks are present in thicker joints and there are multiple fracture origins. Preliminary attempts to heat treat joints to promote crystallization resulted in vaporization of the glass and a low strength.

Further investigations of the interfacial reactions, and room temperature and high temperature strength and fracture mechanisms are planned.

UNCLASSIFIED

SECURITY CLASSIFICATION OF THIS PAGE(When Data Entered)

CONTENTS

	<u>Page</u>
ABSTRACT.....	iii
ILLUSTRATIONS.....	v
SCIENTIFIC CONTRIBUTIONS.....	vii
INTRODUCTION.....	1
EXPERIMENTAL TECHNIQUES.....	3
Materials.....	3
Joining Experiments.....	4
Mechanical Tests.....	4
Reaction Studies.....	4
Microscopy.....	5
RESULTS.....	7
Joining Experiments.....	7
Glass-Si ₃ N ₄ Reactions.....	10
Mechanical Tests.....	18
Mechanisms of Fracture.....	23
Crystallization Studies.....	29
SUMMARY.....	33
FUTURE RESEARCH.....	34
REFERENCES.....	35
PRESENTATIONS.....	36

ILLUSTRATIONS

<u>Figures</u>	<u>Page</u>
1 Boron Nitride Jig Used in Joining Two Pieces of Si_3N_4	5
2 Optical Micrograph of a Thin Joint ($\sim 5 \mu\text{m}$)	8
3 Transition between Si_3N_4 and Glass Joint	9
4 Thermal Expansion Cracks	11
5 Thermal Expansion Cracks and Multiple Fracture Origins on a Fracture Surface	12
6 Schematic Drawing Showing Development of Thermal Expansion Mismatch Cracks in the Joint	13
7 Microstructure of As-Received Si_3N_4 and EDAX Analysis of Glass Pocket (Arrowed)	15
8 Glass Pockets at Increasing Distances from the Joint	16
9 Bright and Dark Field Images of Amorphous (A) and Crystalline (C) Regions Near the Joint	17
10 $\text{Si}_2\text{N}_2\text{O}$ Crystal Growing into Glass from Area of Dissolving SiN_4	19
11 Tensile Surface of a Broken Bend Bar Showing $\text{Si}_2\text{N}_2\text{O}$ Crystals Growing into the Glass	20
12 Fracture Surface in a Thin Joint	21
13 Maximum Strengths of Bars Joined Under Various Conditions	22
14 Strength versus Joint thickness	24
15 Microstructure of a Strong Thin Joint Showing (a) Development of Voids in Joint (b) $\text{Si}_2\text{N}_2\text{O}$ Crystals in Glass	26
16 Fracture Surface in a Thick Joint	27

17	Fracture Surface Showing Origin of Fracture in Glass and Subsequent Fracture Path Through Si_3N_4	28
18	Relative X-ray Diffraction Intensity versus Reaction Time	30
19	Heat Treated Joint Region	31

SCIENTIFIC CONTRIBUTIONS

The project leader is David J. Rowcliffe. Studies of the mechanical behavior and chemical reactions of joined ceramics were performed by Sylvia M. Johnson. The original project leader, Ronald E. Loehman, now with Sandia Laboratories, Albuquerque, performed thermal expansion measurements on the glass. Martha L. Mecartney performed the TEM work at Stanford University under the direction of Robert Sinclair.

INTRODUCTION

The basis for this project was the realization that hot pressed Si_3N_4 could be joined using a glass composition that resembled the composition of the glass found at the grain boundaries. The intergranular phase in liquid phase sintered Si_3N_4 is an oxynitride glass that contains the sintering additives, impurities, and dissolved Si_3N_4 . When an oxide glass is used to join Si_3N_4 , a similar phase should form by the dissolution of Si_3N_4 in the glass. Ideally, the joint region should resemble a grain boundary in the bulk material and have a corresponding strength.

The joining process was investigated during the first year of the project.¹ Glass compositions were selected and the range of conditions for joining was determined. The series of reactions between various forms of Si_3N_4 and the glass chosen for joining were studied by X-ray diffraction (XRD). Microstructural studies of the interface were performed using analytical electron microscopy.

Work during the second year of the project has been divided between continued studies of the chemistry of the system and the physical properties of the joined ceramics. An initial survey of mechanical strength of bars joined under various conditions and with various compositions was performed. The strength was found to be relatively insensitive to the specific joining time and temperature within the optimum range. Studies of the mechanical strength were then concentrated on determining the fracture processes and the significance of the surface finish and joint thickness.

The first year's study of the chemistry of the glass- Si_3N_4 system has continued. The reactions between powders of the two components were followed by XRD, and the nature of the reaction process and products were examined by electron microscopy.

This report discusses the second year's research:

- (1) Evaluation of room temperature mechanical strength of joined pieces.
- (2) Determination of the fracture process by scanning electron microscopy (SEM).
- (3) Studies of the reactions between Si_3N_4 and HN-9M glass, the joining composition.
- (4) Studies of the crystallization behavior of the joint region and of mixtures of Si_3N_4 and glass powders.

EXPERIMENTAL TECHNIQUES

Materials

Two billets of hot pressed Si_3N_4 (NC132-I and NC132-II) and one joining composition, (HN-9M) were used in most tests. The major impurities in the NC132 billets are given in Table 1. NC132-II was used in most strength tests.

Table 1

MAJOR IMPURITIES IN HOT PRESSED SILICON NITRIDE

Si_3N_4 Billet	Impurities(wt%)					
	Mg	O	W	Al	Fe	Ca
NC132*-I	1.25	2.46	4.0	0.15	0.3	0.03
NC132*-II	0.75	2.37	3.5	0.12	0.25	0.12

*Norton Co. Worcester, MA.

The glass composition was as follows:

	wt%		
	SiO_2	MgO	Al_2O_3
HN-9M	54.97	35.26	9.66

Joining Experiments

The sample configuration used initially consisted of two Si_3N_4 plates separated by powdered glass and supported in a boron nitride jig (Figure 1). This configuration produces a simple end seal. The technique has been refined to a two-stage process: an initial glazing step followed by the joining operation. More precise control over the joint thickness can thus be obtained.

Samples are cleaned in trichlorethylene, acetone, and methanol, and a slurry of the powdered (-100#) glass is applied to one piece. Glazing is performed in a graphite furnace under ~ 2 atm N_2 , and temperatures are measured with a Pt-Pt 10% Rh thermocouple. The heat treatment for glazing consists of 15 minutes at 1480°C followed by 10 minutes at 1620°C . The glazed end is ground down until only a thin layer of glass remains, and the glazed piece is then placed above an unglazed piece for joining. The amount of glass left on the glazed piece depends on the desired joint thickness.

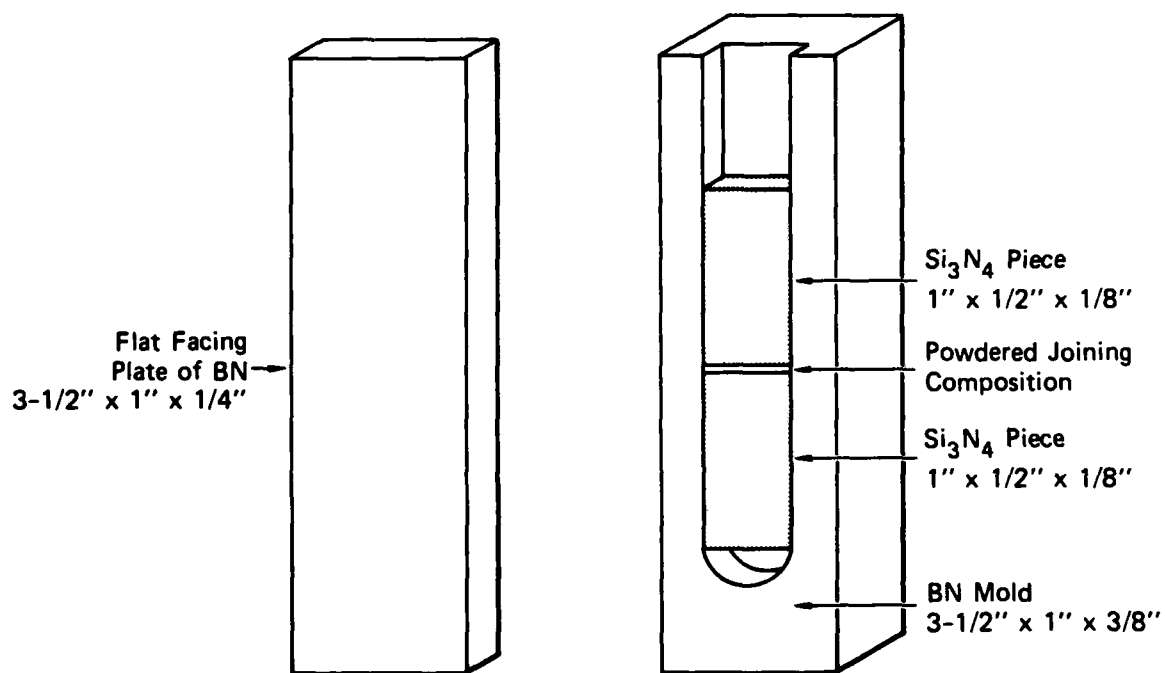
Crystallization treatments were performed on the joined samples immediately after joining.

Mechanical Tests

Joined bars were surface ground and cut into bend test bars ~ 50 mm by 3 mm by 3 mm. Some bars were diamond polished to $1\text{ }\mu\text{m}$ on one face. The edges of the bars were bevelled to remove corner cracks. Joint thicknesses were measured in three places in each sample using a microscope. Samples were broken in a four-point bend configuration with the polished faces in tension.

Reaction Studies

The nature of the reactions in the glass, at the interface and in the Si_3N_4 , were determined by heating mixtures of α , β , amorphous Si_3N_4 powders, and HN-9M glass for various times at 1650°C . The compositions



JA-2527-7

FIGURE 1 BORON NITRIDE JIG USED IN JOINING TWO PIECES OF Si₃N₄

The two pieces of BN are wrapped with molybdenum wire to hold the jig together.

of the reaction products were determined by XRD. Some joints were heat treated for up to 2 hours at 1300°C to promote crystallization.

Microscopy

The joint region in both broken and unbroken bars was examined using SEM. Both the fracture and tensile surfaces of broken bend test bars were studied. A number of joint regions were examined by transmission electron microscopy (TEM) and chemically analyzed using an energy dispersive X-ray system (EDAX).

RESULTS

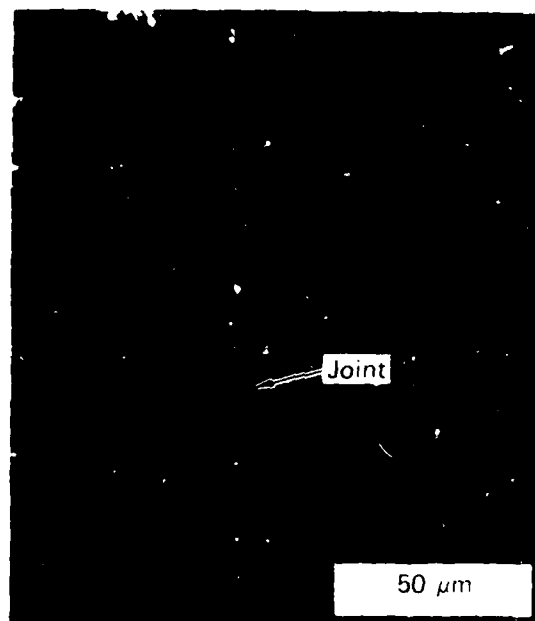
Joining Experiments

Examination of joints produced earlier in this program showed that the thickness of the joined region varied between about 5 and 200 μm , depending on the quantity of glass and the specific joining conditions. Better control of the joining process was obtained when one Si_3N_4 piece was glazed. The glazed layer was then ground down to ensure a plane surface and a minimal amount of glass. However, if all the glass on the surface is removed, leaving only the glass that has penetrated the grain boundaries, the pieces do not join. A minimum amount of glass in the joint is therefore necessary for joining because the glass will not flow out of the grain boundaries.

Part of a very thin ($\sim 5 \mu\text{m}$) joint is shown in Figure 2. The tungsten particles, which appear as white spots in optical and SEM micrographs and as black spots in TEM micrographs, were analyzed by EDAX and were found to contain W, Si, Fe, Co, Cr, and Mn in varying amounts. Similar particles are found in NCl32 hot pressed Si_3N_4 and are known to originate from the WC balls used to mill the powders before hot pressing.

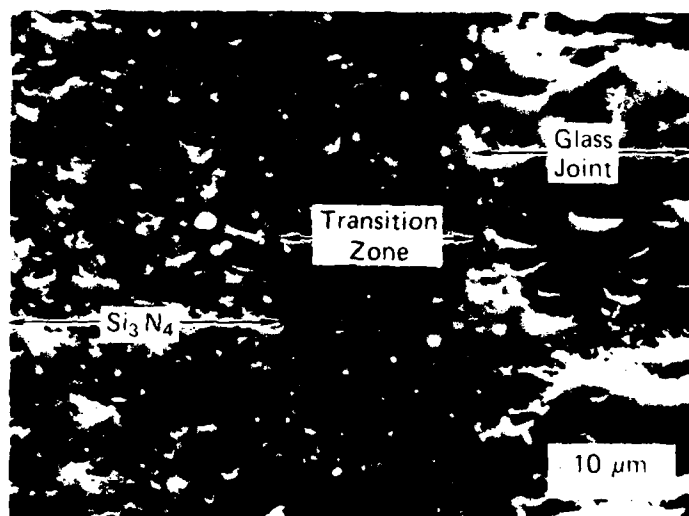
A transition zone between a thicker glass joint and the bulk Si_3N_4 is shown in Figure 3. The glass on the right is damaged during grinding, and even extensive polishing does not completely remove the damage. The damage is aggravated by the cracking, which occurs perpendicular to the joint, and which is thought to be a result of the thermal expansion mismatch.

Si_3N_4 has a thermal expansion coefficient, α , of $\sim 3.2 \times 10^{-6}/^\circ\text{C}$, while HN-9M glass has a thermal expansion coefficient of $\sim 5.96 \times 10^{-6}/^\circ\text{C}$.² The variation in thermal expansion coefficient of HN-9M glass with Si_3N_4 content indicated only a weak dependence of α on the nitrogen content. The coefficient was reduced to $\sim 5.2 \times 10^{-6}/^\circ\text{C}$ in a glass containing 4.3 at% nitrogen.



JP-2527-12

FIGURE 2 OPTICAL MICROGRAPH OF A THIN
JOINT ($\sim 5\mu\text{m}$)



JP-2527-13

FIGURE 3 TRANSITION BETWEEN Si_3N_4 AND GLASS JOINT

The possibility that this difference in expansion coefficients can cause thermal fracture can be estimated as follows.

The strain, e , developed as a result of the mismatch is:

$$e = \Delta\alpha\Delta T \quad (1)$$

With $\Delta T \approx 1000$ K and $\Delta\alpha \approx 2 \times 10^{-6}/^{\circ}\text{C}$, $e \approx 2 \times 10^{-3}$.

The Young's modulus of HN-9N glass was determined by an acoustic resonance technique to be ~ 140 GPa. The stress, σ_{α} , which develops in the glass as a result of the thermal expansion difference, is thus ~ 280 MPa. The strength of the glass at room temperature was measured to be ~ 175 MPa. Therefore, the thermal expansion mismatch stress is sufficient to cause the observed cracking.

Examples of thermal expansion mismatch cracks can be seen in Figures 4 and 5. The cracks are perpendicular to the plane of the joint (Figure 4) and develop in the glass. The traces of these cracks can be seen on fractured surfaces where the glass has broken into many small pieces (Figure 5). The cracks, represented schematically in Figure 6, extend into the transition zone which contains a large amount of glass. There are no cracks parallel to the joint because the upper Si_3N_4 piece is free to move and relieve any no stress perpendicular to the joint. The cracks and their role in the fracture process are discussed in more detail below.

The glass is not as hard or as tough as the Si_3N_4 and tends to chip out along these cracks during grinding. The visible transition zone in Figure 3 is ~ 30 μm wide and appears to be less pitted than the Si_3N_4 , indicating that glass from the joint has penetrated at least that far into the bulk.

Glass- Si_3N_4 Reactions

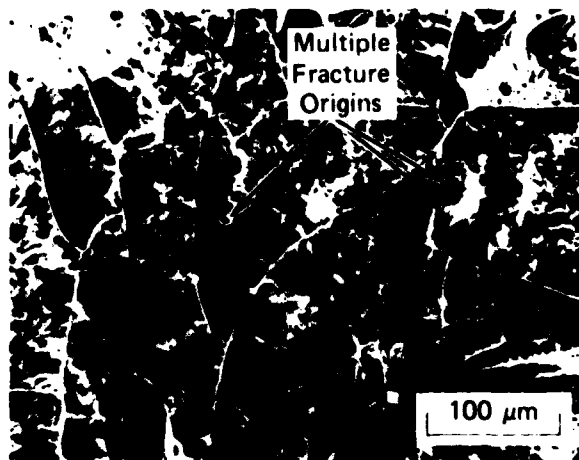
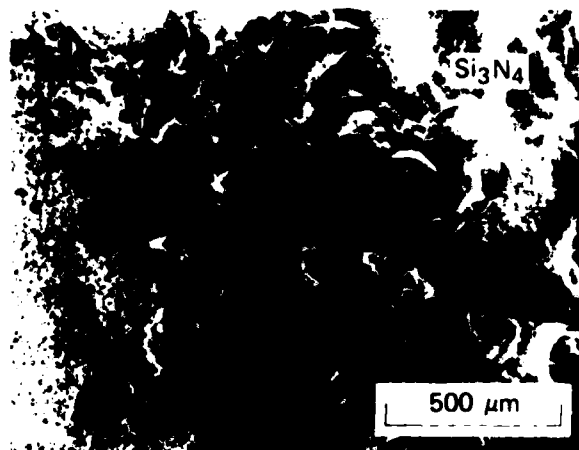
The reaction between the glass and the Si_3N_4 appears to proceed as previously described: glass penetrates the Si_3N_4 grain boundaries, and Si_3N_4 starts to dissolve in the glass, precipitating $\text{Si}_2\text{N}_2\text{O}$, a metastable



Thermal
Expansion
Cracks

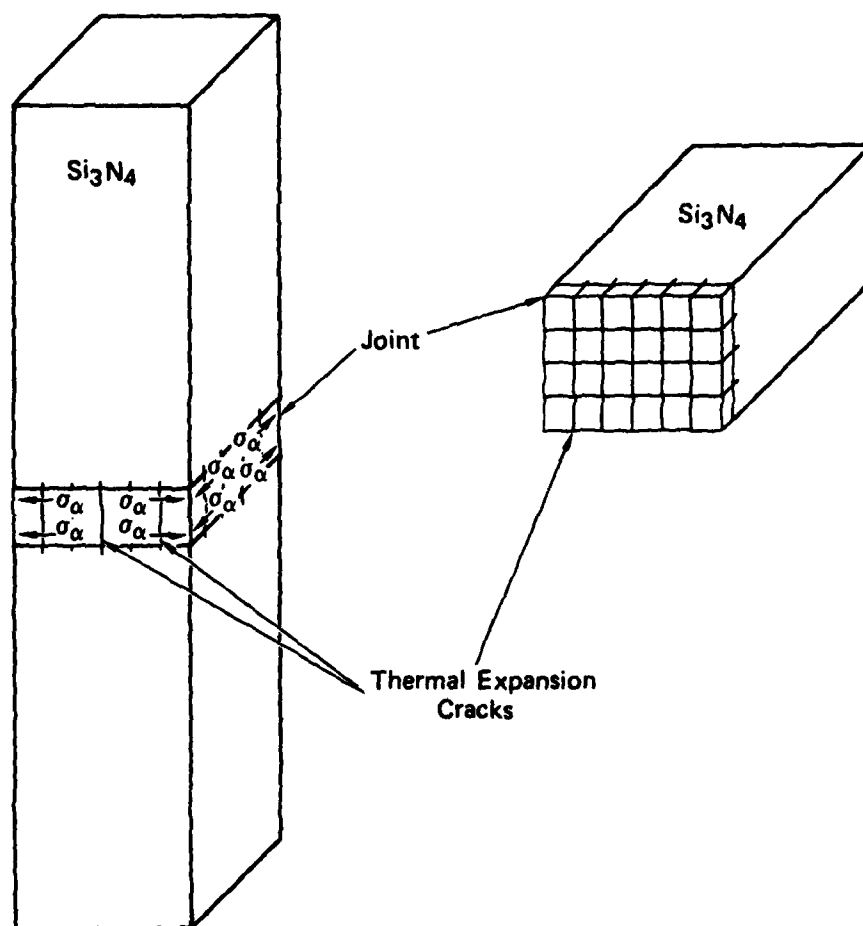
JP-2527-14

FIGURE 4



JP-2527-17

FIGURE 5 THERMAL EXPANSION CRACKS AND MULTIPLE FRACTURE ORIGINS ON A FRACTURE SURFACE



JA-2527-15

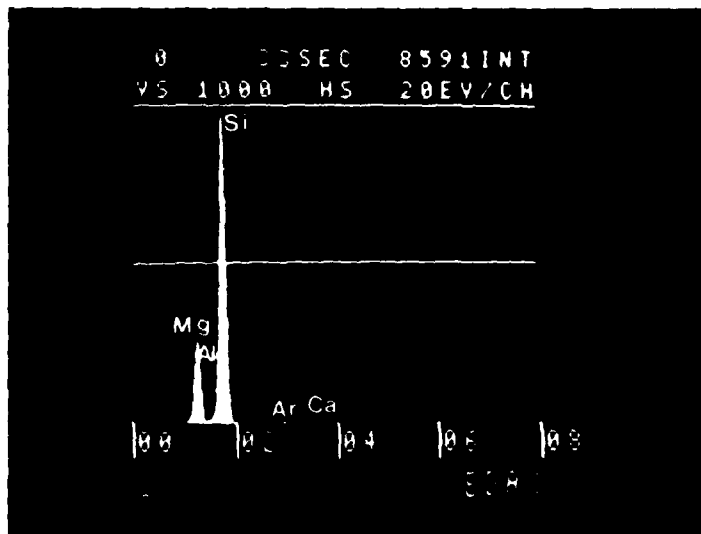
FIGURE 8 SCHEMATIC DRAWING SHOWING DEVELOPMENT OF THERMAL EXPANSION MISMATCH CRACKS IN THE JOINT

phase. Silicon oxynitride crystallizes from the glass as increasing amounts of Si_3N_4 dissolve. Eventually the rate of $\text{Si}_2\text{N}_2\text{O}$ crystallization should decrease, and Si_3N_4 should reform as an equilibrium phase.¹ However, reprecipitated Si_3N_4 has not been observed in any of the joints, and its formation is probably precluded by the relatively rapid vaporization of the glass. The reactions have been studied using both electron microscopy of the joint regions and X-ray analysis of the phases formed in mixtures of Si_3N_4 and glass powders heated for various times to model the reactions. After long periods (4 hours) at 1650°C, the final phase was $\beta\text{-Si}_3\text{N}_4$ in predominantly Si_3N_4 mixtures. Mixtures originally containing 85% HN-9M glass were amorphous after long annealing periods.

The microstructure of the as-received Si_3N_4 is shown in Figure 7, with an EDAX analysis of one of the large ($\sim 1000 \text{ \AA}$) glass pockets. The weight ratio of the Si:Mg:Al:Ca in the glass is 1.0:0.42:0.02:0.001. The Si content in the glass appears high, but this is probably a result of the size of the electron beam being larger than the glass pocket. For comparison, a typical EDAX analysis of the glass in a joint gives a Si:Mg:Al ratio of 1:0.78:0.11, whereas the calculated ratio in HN-9M glass is 1:0.81:0.12.

Lanthanum and scandium were added separately to the glass to act as tracers. Approximately 13 wt% Sc or 5 wt% La were substituted for Mg in the glass composition. Glass penetration could not be traced by the microprobe because the background interference was too great. Therefore, TEM and EDAX were used to find and analyze glass pockets at increasing distances from the joint (Figure 8). The size of the glass pockets decreases with increasing distance from the joint, although the pocket size varies at greatly identical distances from the joint. Scandium was detected as far as 0.7 mm from the joint.

Crystallization of some glass pockets in samples joined with HN-9M-13 wt% Sc glass was observed [Figure 8(c)]. Amorphous (A) and crystallized (C) pockets near the joint region are shown in Figure 9. EDAX analyses of crystallized regions both near and far from the joint indicate that they

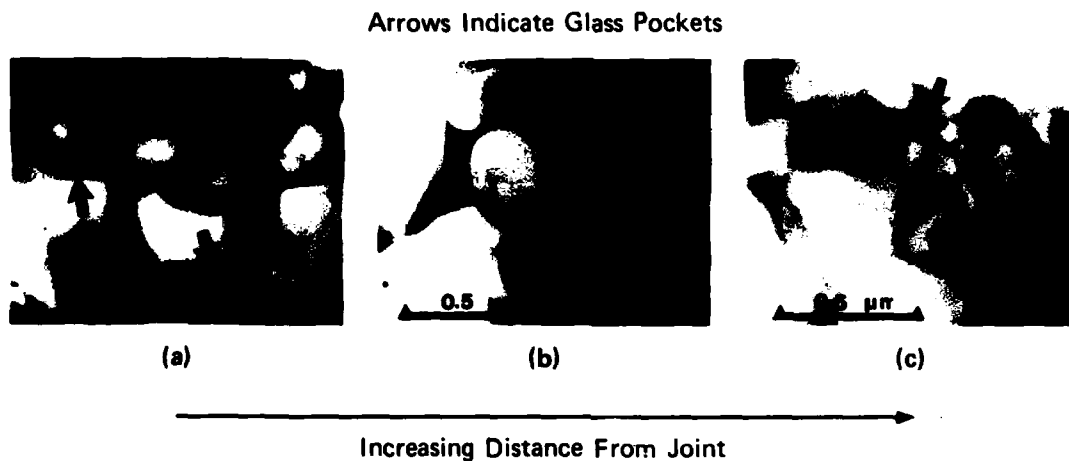


Normalized Composition

Si	Mg	Al	Ca
1.0	0.42	0.02	0.001

JP-2527-16

FIGURE 7 MICROSTRUCTURE OF AS-RECEIVED Si_3N_4 AND EDAX ANALYSIS OF GLASS POCKET (ARROWED)



	Distance From Joint, mm	Approximate Glass Pocket Size, μm	Elemental Analysis of Glass Pockets*			
			Si	Mg	Al	Sc
	0		1	0.73	0.15	0.15
(a)	0.15	0.5-1	1	0.77	0.13	0.13
(b)	0.45	0.25-0.5	1	0.78	0.07	0.04
(c)	0.70	0.1-0.2	1	0.62	0.04	0.007

*Normalized to Si = 1

JP-2527-18

FIGURE 8 GLASS POCKETS AT INCREASING DISTANCES FROM THE JOINT
Table gives normalized elemental analyses of the glass pockets.



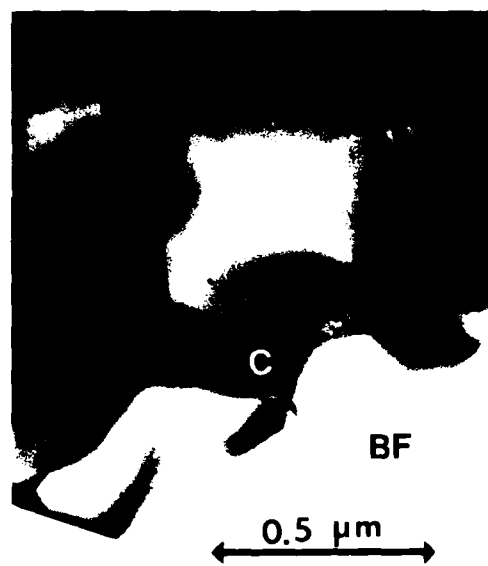
(a)



(b)



(c)



(d)

BF—Bright Field
DF—Dark Field
A—Amorphous
C—Crystalline

JP-2527-19

FIGURE 9 BRIGHT AND DARK FIELD IMAGES OF AMORPHOUS (A) AND CRYSTALLINE (C) REGIONS NEAR THE JOINT

Si_3N_4 grains are dissolving in large glass pocket in (a)

have increased magnesium and slightly reduced aluminum contents. Crystallization was only observed in scandium-containing glasses.

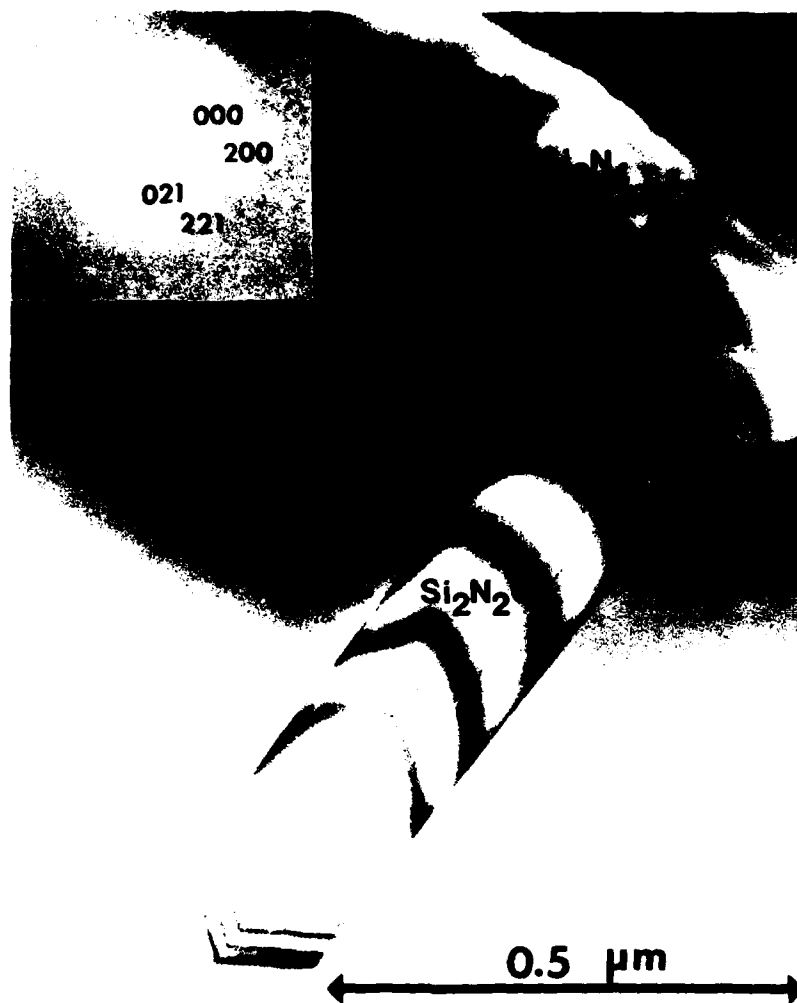
Silicon nitride crystals dissolving in the glass can be seen in the dark field image, Figure 9(a). Dissolution of Si_3N_4 is followed by precipitation of acicular $\text{Si}_2\text{N}_2\text{O}$ crystals. Figure 10 shows a $\text{Si}_2\text{N}_2\text{O}$ crystal growing into the glass from an area containing a dissolving Si_3N_4 grain. The acicular shape is characteristic of $\text{Si}_2\text{N}_2\text{O}$ grown under these conditions. The identification is confirmed by the selected area electron diffraction pattern shown in Figure 10. $\text{Si}_2\text{N}_2\text{O}$ crystals of up to 15 μm were observed using both TEM and SEM.

$\text{Si}_2\text{N}_2\text{O}$ crystals can also be observed using SEM. Figure 11 shows the polished, tensile surface of a broken bend bar. The light crystals growing into the glass from the Si_3N_4 are $\text{Si}_2\text{N}_2\text{O}$. Large glass pockets can also be seen in the interfacial region. Tungsten particles, which indicate the original position of the interface, can be seen in the glass above the level of the $\text{Si}_2\text{N}_2\text{O}$ crystals, indicating the extent of Si_3N_4 dissolution.

The interlocking nature of the $\text{Si}_2\text{N}_2\text{O}$ crystals is shown in Figure 12, which shows part of the fracture surface through a thin joint. Very little glass remains, and the $\text{Si}_2\text{N}_2\text{O}$ layer is very porous. This is a result of the ~ 12-15% volume change associated with $\text{Si}_2\text{N}_2\text{O}$ crystallization and removal of the glass by diffusion along the grain boundaries in the Si_3N_4 . The volume change results from the difference in densities³ between $\text{Si}_2\text{N}_2\text{O}$ (~ 2.87 g/cm³) and oxynitride glasses (~ 2.6/cm³). As $\text{Si}_2\text{N}_2\text{O}$ crystals grow, holes form in the surrounding glass. Part of the fracture path through Si_3N_4 is also shown in Figure 12 for comparison.

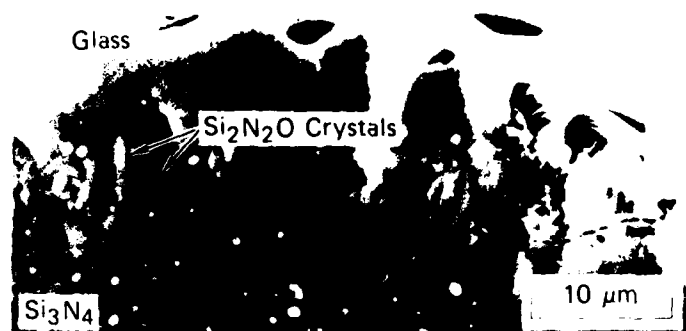
Mechanical Tests

Four-point bend tests were used to determine the strength of joints from the first experiments and to define a set of optimum joining conditions. Various glass compositions and two silicon nitrides were used in these initial tests. The joint thickness was not controlled in these early experiments and nor were the test bars were polished. The results



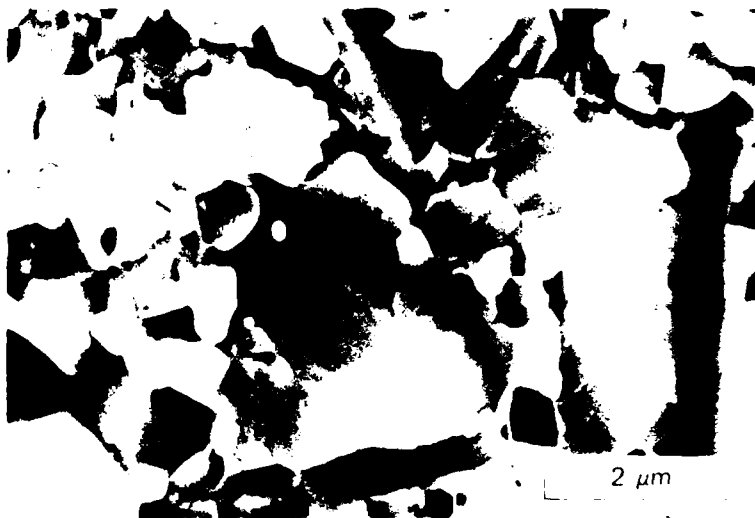
JP-2527-20

FIGURE 10 $\text{Si}_2\text{N}_2\text{O}$ CRYSTAL GROWING INTO GLASS FROM
AREA OF DISSOLVING SiN_4

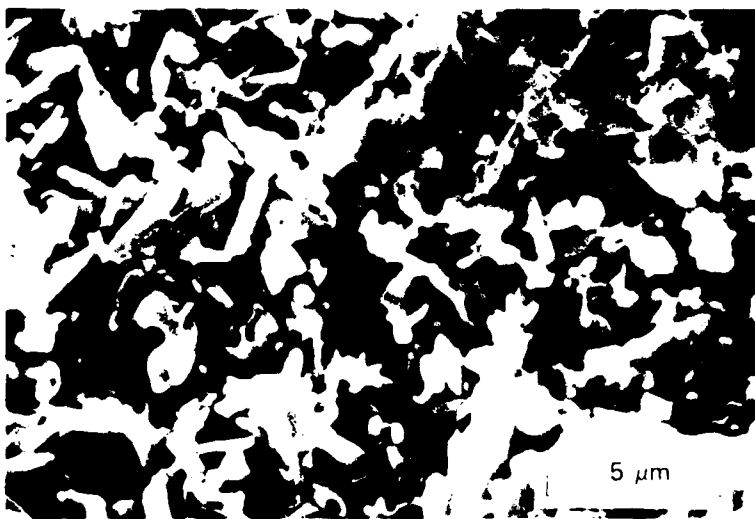


JP-2527-21

FIGURE 11 TENSILE SURFACE OF A BROKEN BEND BAR
SHOWING Si₂N₂O CRYSTALS GROWING INTO
THE GLASS



(a) Fracture through Si_3N_4



(b) Fracture through interlocking $\text{Si}_2\text{N}_2\text{O}$ crystals

JP-2527-22

FIGURE 12 FRACTURE SURFACES IN A THIN JOINT.

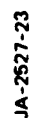


FIGURE 13 MAXIMUM STRENGTHS OF BARS JOINED UNDER VARIOUS CONDITIONS

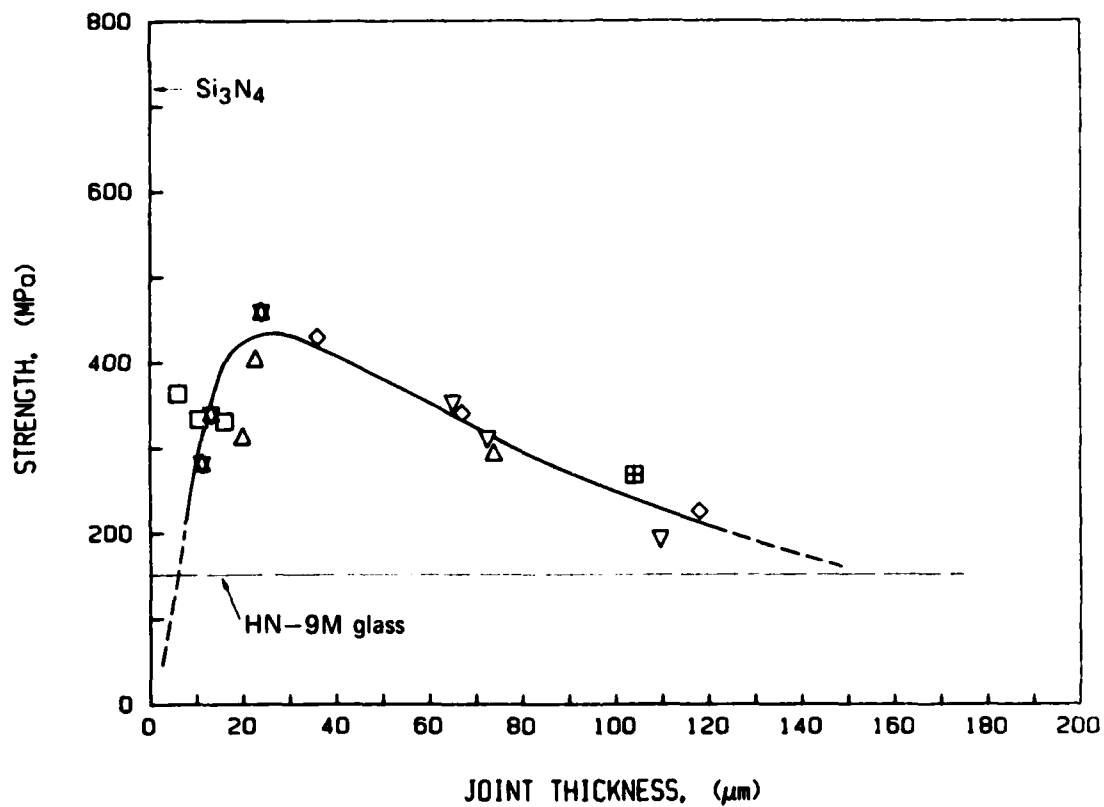
of the initial strength survey are shown in Figure 13. Only the maximum strengths obtained are plotted because these represent the best strengths attainable. However, within the optimal range of joining conditions, 1575-1650°C and 30 to 60 minutes, the strengths are clustered around ~ 400 MPa and do not appear to depend on the specific joining condition. Outside the optimum range, the strengths are very low and bars break during normal handling. The strength of Si_3N_4 bars is ~ 725 MPa and of glass bars is ~ 175 MPa.

As the maximum strengths appeared to be independent of joining conditions, one set of joining conditions, 1580°C for 45 minutes, was chosen for strength tests. A method of polishing joined bars to 1 μm was devised to remove the surface damage associated with grinding. Joint thickness can be more easily measured on polished surfaces, and the joint region can be examined by SEM. Several bars were joined under identical conditions, polished, and the strengths measured. The fracture and tensile surfaces of a number were examined by SEM. The fracture origins are nearly always subsurface, and there was no difference in strength between polished and ground samples.

The fracture strengths, as a function of joint thickness, are plotted in Figure 14. The shape of the strength-joint thickness curve suggests that there are two fracture mechanisms. The strength increases with joint thickness from joint thicknesses below ~ 20-25 μm and decreases with increasing joint thickness above ~ 35 μm . The strength is relatively constant within the transition zone of ~ 25-35 μm . the maximum strength achieved is ~ 460 MPa.

Mechanisms of Fracture

SEM examination of the fracture surfaces indicates that there are indeed two fracture mechanisms. If a joint is very thin, < ~ 25 μm , $\text{Si}_2\text{N}_2\text{O}$ crystals will grow across the joint and form an interlocking array. However, the glass is consumed during crystal growth, and the resulting structure is very porous as is shown in Figure 12. Fracture initiates in the $\text{Si}_2\text{N}_2\text{O}$ layer and the crack travels through the $\text{Si}_2\text{N}_2\text{O}$,



JA-2527-24

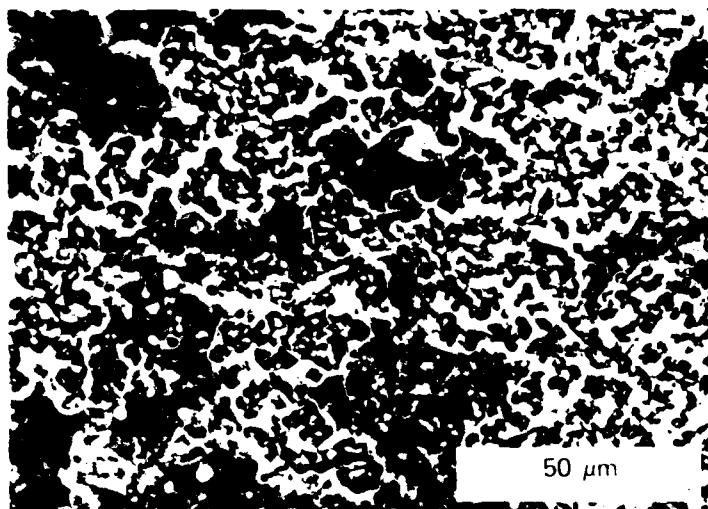
FIGURE 14 STRENGTH VERSUS JOINT THICKNESS

Joining conditions were 1580°C for 45 minutes under 2 atm N₂.
Like symbols indicate test bars cut from a single joined specimen.

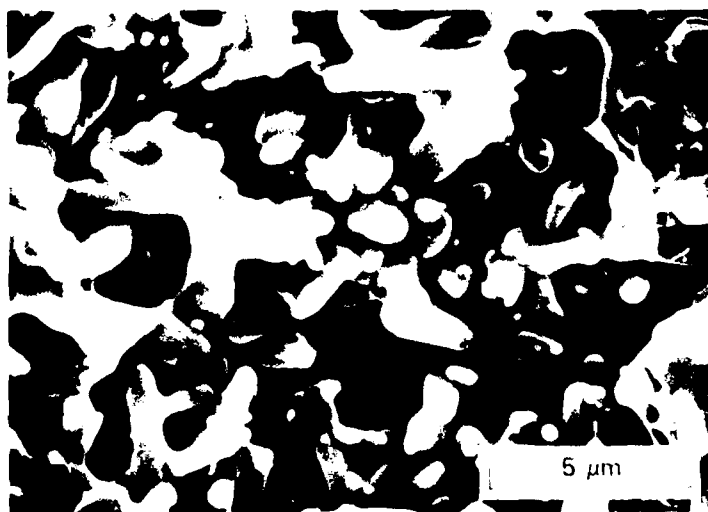
the interface, and the Si_3N_4 . The strengths are low as a result of the porosity of the interfacial layer. As the joint thickness increases, more glass will remain between the $\text{Si}_2\text{N}_2\text{O}$ crystals. The crack path will be partially through these glassy areas and will be deflected by the $\text{Si}_2\text{N}_2\text{O}$ crystals. An example of the microstructure of a higher strength joint is shown in Figure 15, where $\text{Si}_2\text{N}_2\text{O}$ crystals have grown in the glass. However, some areas are becoming porous as the glass is consumed. The low strength of very thin joints can probably be attributed to incomplete glass coverage of the Si_3N_4 and the subsequent formation of large voids in the joint.

Thicker joints, $> \sim 35 \mu\text{m}$, contain more glass, and $\text{Si}_2\text{N}_2\text{O}$ crystals are unable to grow completely across the joint. $\text{Si}_2\text{N}_2\text{O}$ crystals do grow across the Si_3N_4 -glass interface, resulting in a strong interfacial bond. The layer of glass in a thick joint cracks as a result of the thermal expansion mismatch. These cracks run through the interface but only penetrate a short distance into the Si_3N_4 . Large glass pockets are present in the Si_3N_4 near the joint and the cracks only extend into those regions. The thermal expansion cracks can be seen in Figure 5 and, as a result of the many essentially independent areas formed, there are multiple fracture origins.

The independent fracture initiation sites are often bubbles or pores in the glass. Cracks grow across each of these areas but stop at the thermal expansion cracks. Eventually, many adjoining areas fracture and catastrophic failure occurs. When a developing crack intersects a pre-existing crack, it tends to restart at the ends of that crack and to continue through the Si_3N_4 . Cracks may run along the interface for short distances but are deflected by the $\text{Si}_2\text{N}_2\text{O}$ crystals. However, if the $\text{Si}_2\text{N}_2\text{O}$ crystals are very small, ($< \sim 3 \mu\text{m}$) the crack may not be substantially deflected from its path (Figure 16). Higher strengths are associated with a major portion of the crack path running through the Si_3N_4 . Figure 17 shows an example of a high strength sample where the fracture origin is in the glass but the fracture path is mostly through Si_3N_4 .



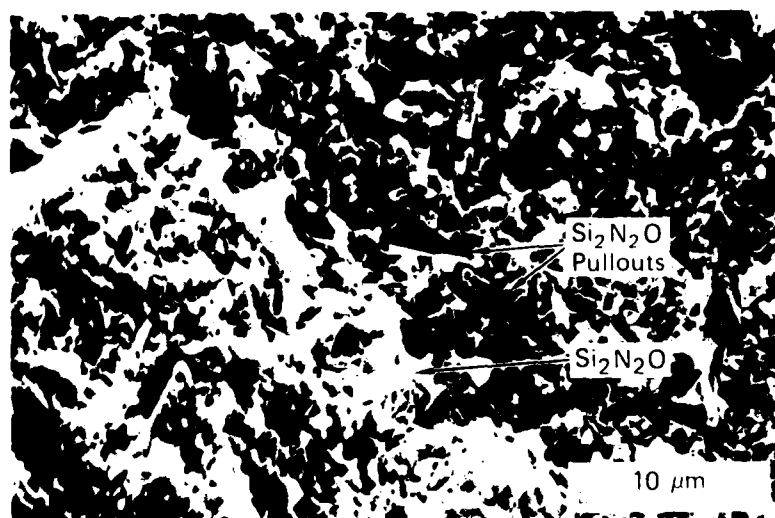
(a)



(b)

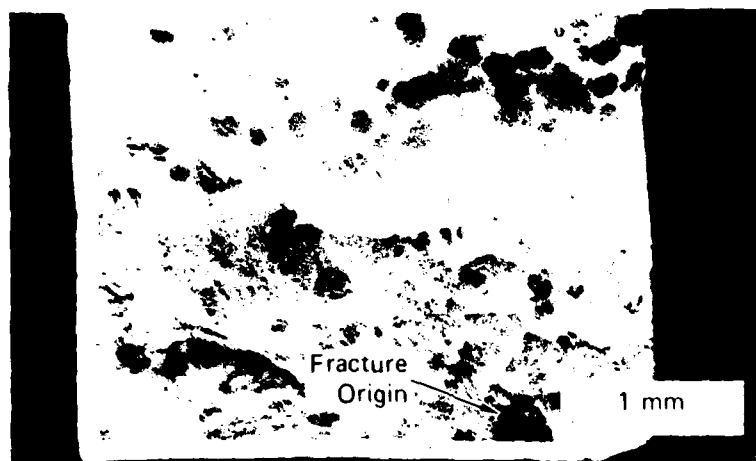
JP-2527-25

FIGURE 15 MICROSTRUCTURE OF A STRONG THIN JOINT
SHOWING (a) DEVELOPMENT OF VOIDS IN
JOINT (b) $\text{Si}_2\text{N}_2\text{O}$ CRYSTALS IN GLASS

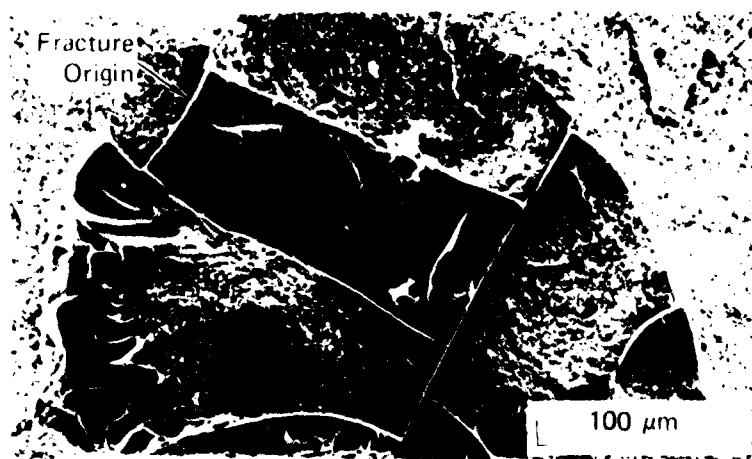


JP-2527-26

FIGURE 16 FRACTURE SURFACE IN A THICK JOINT
Note pulls out and $\text{Si}_2\text{N}_2\text{O}$ crystals.



(a)



(b)

JP-2527-27

FIGURE 17 FRACTURE SURFACE SHOWING ORIGIN OF FRACTURE
IN GLASS AND SUBSEQUENT FRACTURE PATH
THROUGH Si_3N_4

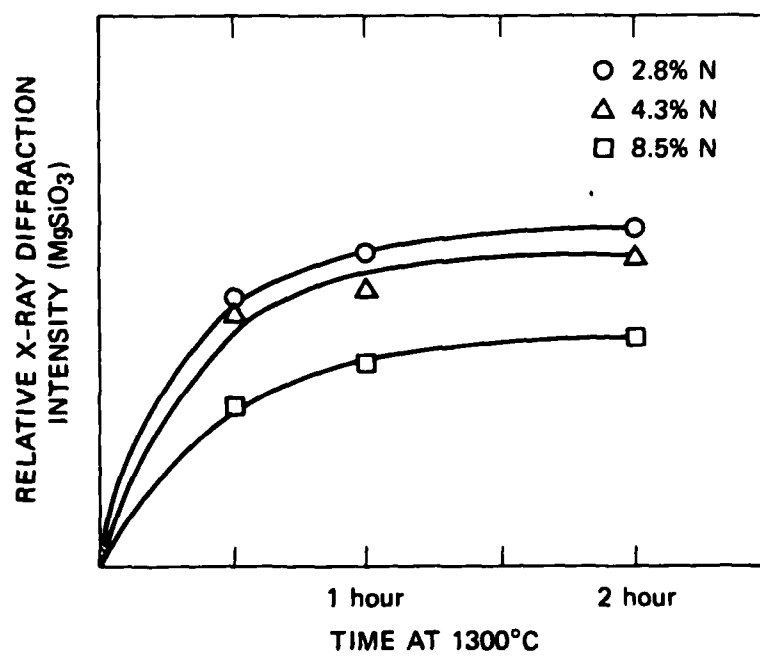
There is a transition region where the two fracture mechanisms occur simultaneously, i.e., some areas of the joint are cracked and others only have $\text{Si}_2\text{N}_2\text{O}$ crystals present. An ideal joint would have $\text{Si}_2\text{N}_2\text{O}$ crystals growing across the joint but in a glass matrix. The crystals would toughen the glass and increase the strength. Moreover, a joint microstructure of this type will only form within a very limited joint thickness range, and thus control over the amount of glass used in glazing and joining is critical. However, a range of joint thicknesses for a desired strength can be defined from the present results, i.e., within certain minimum and maximum thickness limits the joint will have a certain strength regardless of the pertinent fracture mechanism.

Crystallization Studies

Crystallization studies were performed on joined bars and on mixtures of HN-9M glass and Si_3N_4 powders to simulate conditions at the interface. The maximum amount of Si_3N_4 that will dissolve in HN-9M glass was found to be ~ 12-15 wt%. Frothing occurred with larger amounts of Si_3N_4 and the resultant samples were not amorphous, even when cooled rapidly.

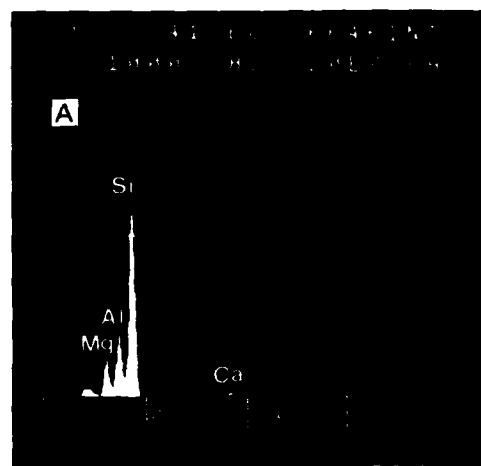
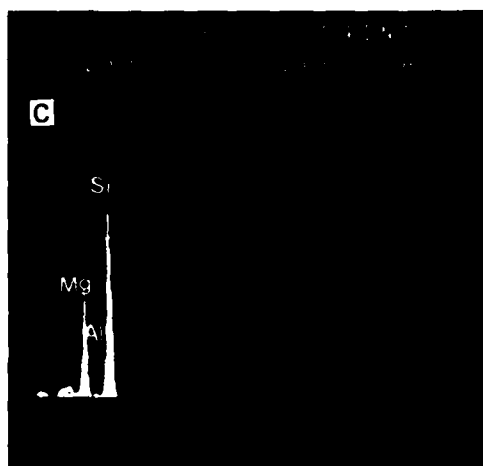
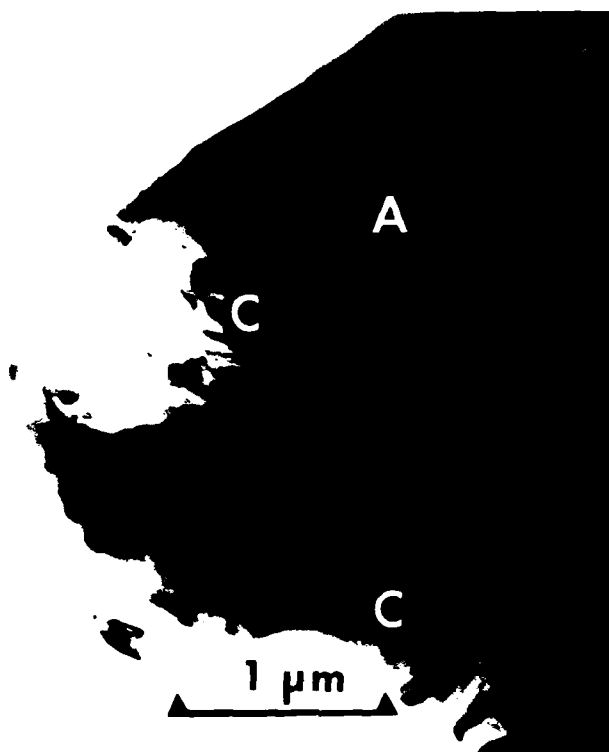
Glass Si_3N_4 mixtures containing 5, 7.5 and 15 wt% Si_3N_4 (2.8, 4.3, and 8.5 at% N) were reacted at 1650°C for 1 hour in N_2 and rapidly cooled. The resulting samples were completely amorphous and were subsequently heat treated at 1300°C for various times. The major crystalline phase to precipitate was MgSiO_3 . The amount of MgSiO_3 that crystallized increased with increasing time at temperature (Figure 18), reaching a steady state value after ~ 2 hours. The amount of precipitated MgSiO_3 decreased as the nitrogen content increased.

The joint region of a specimen joined at 1550°C for 30 minutes followed by a heat treatment at 1300°C for 90 minutes was examined using TEM. The joint was partially crystallized (Figure 19) and an analysis of the crystalline regions showed that Si and Mg were the major constituents, indicating that the crystalline phase is MgSiO_3 . Conversely, the amorphous regions had decreased Mg and increased Al content, indicating initial phase separation followed by crystallization of MgSiO_3 . The bend



JA-2527-28

FIGURE 18 RELATIVE X-RAY DIFFRACTION INTENSITY VERSUS REACTION TIME



JP-2527-29

FIGURE 19 HEAT TREATED JOINT REGION
Joint is partially crystalline (C)
and partially amorphous (A)

contours in the crystalline phase indicate that this phase is highly strained.

Some samples were heat treated to determine the effect of crystallization on the strength. Long heat treatments (~ 6 hours) caused the glass to disappear. Bend tests on a set of samples joined at 1580°C for 45 minutes and subsequently heat treated at 1300°C for 2 hours revealed very low strengths which were of the order of the strength of HN-9M glass. These tests are being continued.

SUMMARY

The joining technique developed during the first year of the project was refined during the second year and now includes a glazing step.

Glazing before joining allows better control of the process, which results in a thinner, more uniform joint. The reactions at the joint were simulated with mixtures of various forms of Si_3N_4 and glass powders. The enhanced reaction rate obtained with powder mixtures means that the entire reaction series could be determined. The reactions at the joint occur more slowly and are not complete, i.e., Si_3N_4 was not observed to precipitate in the joints. TEM and EDAX analysis were used to study the interfacial reactions and extent of glass penetration into Si_3N_4 .

A preliminary survey of joint strengths indicated that the strength was independent of the joining time and temperature within the optimum range of 30-60 minutes and 1575-1650°C. Two fracture modes were identified by SEM and linked to the joint thickness and extent of interfacial reaction. The thermal expansion mismatch between the glass and Si_3N_4 and the resulting cracks appeared to influence the fracture process greatly. The thermal expansion coefficients, α , of various glass compositions were measured; α is only weakly dependent on the nitrogen content.

The extent of crystallization of Si_3N_4 -glass powder mixtures is dependent on the nitrogen content. MgSiO_3 was the major crystalline phase found in crystallized regions.

FUTURE RESEARCH

During the next contract year substantial attention will be paid to understanding the fracture process at room temperature and to investigating mechanical properties high temperature. Chemical aspects of the joint region will continue to be investigated by TEM and XRD.

The following tasks are planned for the next contract year:

- Correlate joining conditions strength, joint thickness, and fracture mode by 4 point bend tests and SEM.
- Make further measurements of the strength of heat-treated joints and joints made using glasses with different thermal expansion coefficients to determine the role and significance the thermal expansion mismatch cracks on the strength.
- Study the high temperature mechanical strength of the bonds and analyze the fracture process using SEM.
- Continue TEM studies of the interfacial reactions.
- Measure the fracture toughness and strength of indented bars.
- Model the stress-joint thickness-thermal expansion coefficient relationships and predict the maximum possible strength of a joint in Si_3N_4 .

REFERENCES

1. R. E. Loehman, M. L. Mecartney, and D. J. Rowcliffe, "Silicon Nitride Joining," AFOSR Annual Report, Contract No. F49620-81-K-0001, February, 1982.
2. R. E. Loehman, private communication, (1983).
3. I. Idrestedt and C. Brossett, Acta Chem. Scand. 18 (8), 1879-1886 (1964).

PRESENTATIONS

1. D. J. Rowcliffe, R. E. Loehman, and M. L. Mecartney "Structure of Silicon Nitride Joints," American Ceramic Society Annual Meeting, Cincinnati, OH, May 1982.
2. M. L. Mecartney, R. Sinclair, D. J. Rowcliffe, and R. E. Loehman, "Interfacial Reactions in Joined Silicon Nitride," American Ceramic Society Pacific Coast Meeting, Seattle, WA, October 1982.
3. D. J. Rowcliffe, "Structural Ceramics in Heat Engines," Invited Seminar at Lockheed Palo Alto Research Laboratory, February 1983.